arXiv:1407.3628v1 [nucl-ex] 14 Jul 2014

Multiple Parton Interactions with ALICE: from pp to p–Pb

Andreas Morsch
for the ALICE Collaboration
CERN, 1211 Geneva, Switzerland
E-mail: andreas.morsch@cern.ch

Abstract. The study of multiplicity dependent di-hadron angular correlations allows us to assess the contribution of multiple-parton interactions to particle production. We will review these measurements in pp and p–Pb collisions with the ALICE detector at the LHC and discuss the results in the context of centrality determination and other multiplicity dependent observables in p–Pb.

1. Introduction

The concept of multiple parton–parton interactions (MPI) provides the theoretical basis to understand global event properties of non-diffractive, minimum bias pp collisions. The model also allows for a straightforward interpretation of the fact that at high $\sqrt{s}$ the leading order cross-section for $2 \to 2$ parton scatterings with momentum transfer $Q > Q_{\rm min} \gg \Lambda_{\rm QCD}$ exceeds the total pp cross-section at a range of $Q_{\rm min}$-values where perturbative QCD is applicable [1]. At LHC energies, this happens already at $Q_{\rm min} \approx 4$ GeV/c [2, 3, 4]. In a naive factorisation approach the mean number of scatterings per event ($n_{\rm hard}$) is equal to the ratio of the hard and the total cross-section, $\sigma_{\rm hard}/\sigma_{\rm tot}$. In more realistic phenomenological models like PYTHIA6 [5], PYTHIA8 [6] and HERWIG++ [4], the colour screening effect regularises the divergence ($\propto 1/p_{\rm T}^4$) of the hard cross-section at low $p_{\rm T}$ (< 2 GeV/c). Moreover, being limited by energy and momentum conservation $n_{\rm hard}$ can not reach arbitrarily large values. In particular, these models implement a pp impact parameter dependence which explains the so called jet-pedestal effect in the underlying event of hard collisions [7].

The underlying event is conventionally defined as the region transverse to the leading jet or particle in an event, $\pi/3 < |\Delta\varphi| < 2\pi/3$, where $\Delta\varphi$ is the azimuthal distance to the leading object. Figure 1 shows for pp collisions at $\sqrt{s} = 7$ TeV the measured charged particle density in the transverse region as a function of the leading particle transverse momentum ($p_{\rm T}$) [8]. The particle density exhibits a steep rise at low $p_{\rm T}$ until $p_{\rm T} \approx 4$ GeV/c where a plateau is reached. In the framework of MPI, events with a higher leading particle $p_{\rm T}$ correspond to more central pp collisions in which the probability for additional uncorrelated hard scatterings is enhanced. This effect is also well known in nucleus–nucleus collisions and described by the proportionality of the yield from hard processes to the nuclear overlap function. For example, in Pb–Pb collisions about half of yield of particles or jets from hard processes is found in the 10% most central collisions. Consequently selecting high-$p_{\rm T}$ particles one selects also preferentially more central collisions until a maximal centrality bias is reached.

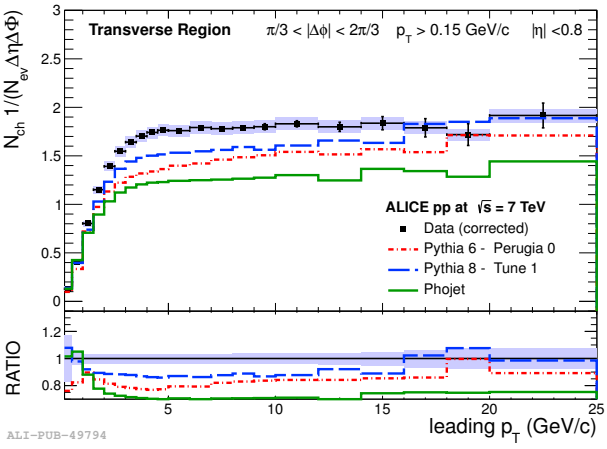

Figure 1. Number density in the transverse region of leading particles as the function of the leading particle p_{T} for pp collisions at $\sqrt{s} = 7$ TeV [8].

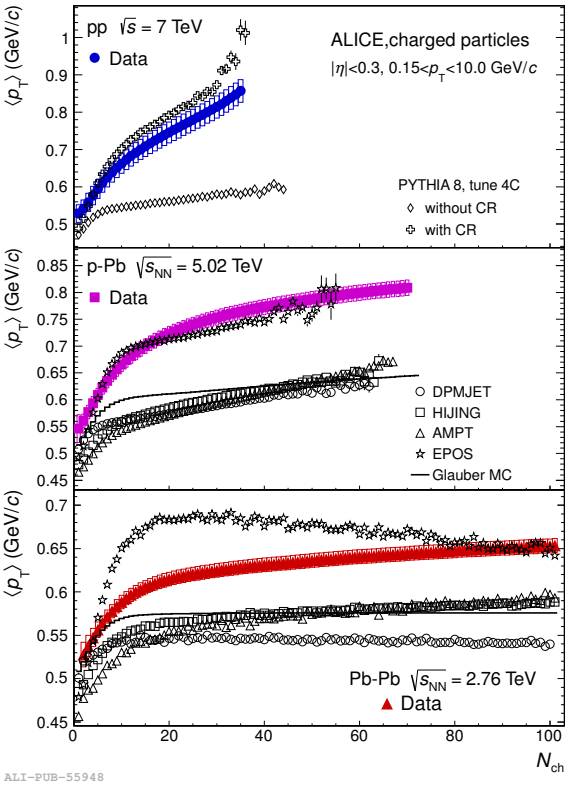

Figure 2. The mean particle transverse momentum as a function of multiplicity in $|\eta| < 0.3$ for pp collisions at $\sqrt{s} = 7$ TeV (upper panel), p–Pb collisions at $\sqrt{s_{\mathrm{NN}}} = 5.02$ TeV (middle panel) and Pb–Pb collisions at $\sqrt{s_{\mathrm{NN}}} = 2.76$ TeV (lower panel) [11].

Coherence effects between multiple scatterings, called colour re-connections (CR), have been introduced in order to explain the steep rise of the particle mean p_{T} as a function of the event multiplicity N_{ch} observed in pp collision [9, 10]. Figure 2 (upper panel) shows the measured $\langle p_{\mathrm{T}} \rangle (N_{\mathrm{ch}})$ compared to the results from PYTHIA8 simulations with and without CR [11]. The model without CR clearly fails to describe the data, whereas by including this effect the agreement is quite good. The EPOS LHC Monte Carlo generator [12] which includes collective hydrodynamic flow for small systems like pp, is also in good agreement with $\langle p_{\mathrm{T}} \rangle (N_{\mathrm{ch}})$ and the underlying event measurements at the LHC.

At LHC energies, the large number of initial hard parton–parton scatterings is a common feature of high-multiplicity pp, p–Pb and Pb–Pb collisions. In the MPI model, high-multiplicity pp collisions arise from low-impact parameter collisions and statistical upward fluctuations of the number of MPIs per event. Depending on the position and width of the pseudorapidity (η) window $\Delta\eta$ in which multiplicity is counted these events are also expected to contain harder than average partonic collisions and with partons fragmenting into a larger than average number of hadrons (fragmentation bias). In Pb–Pb, the mean number of initial parton–parton scatterings is determined almost entirely by the collision centrality. Additional biases are weak. Proton-lead collisions can be expected to lie in between these two cases. In models that treat p–Pb collisions as independent p–N collisions, the number of parton–parton scatterings is expected to

be determined by the p–Pb and p–N centralities. Therefore a detailed insight into MPI related effects in pp collisions is needed to understand pp as a reference for p–Pb.

2. The structure of high multiplicity pp collisions

Two-Particle Azimuthal Correlations

Two-Particle azimuthal correlations represent a powerful tool to understand the origin of high-multiplicity pp collisions. Such studies involve measuring the distributions of the relative azimuthal angle $\Delta\varphi$ between pairs of particles: a "trigger" particle in a certain transverse momentum $p_{\mathrm{T,trig}}$-interval and an "associated" particle in a $p_{\mathrm{T,assoc}}$-interval. In these correlations, the fragmentation products of parton-parton scatterings manifest themselves as characteristic near-side ($\Delta\varphi = 0$) peak- and away-side ($\Delta\varphi = \pi$) ridge-structures. The number of correlated particles per trigger particle is defined as the yield of particles in the peaks over the uncorrelated background which is constant in $\Delta\varphi$. In models describing high-multiplicity pp events as superpositions of multiple scatterings this normalised yield is expected to be constant or to increase as a function of multiplicity. In the case where a soft component in the p_{T}-range of the trigger becomes dominant at high multiplicities, the yield per trigger-particle decreases.

In pp collisions at LHC energies, an increase of the near- and away-side yields as a function of the charged particle multiplicity is observed (see Fig. 3) [13]. This rise is well described by recent PYTHIA6 tunes and PYTHIA8 and in these models it is due to the increase of the number of MPIs and the increase of the average Q^2 of the collisions. The number of observed trigger particles depends on the number of initial partons and the number of fragments per parton. Since the latter rises with multiplicity, a non linear increase of the number of trigger particles with multiplicity is observed. Hence, the number of trigger particles is not a good measure of the number of MPIs contributing to the event multiplicity.

In order to reduce the sensitivity to parton fragmentation, ALICE studies the number of uncorrelated seeds ($N_{\mathrm{uncorrelated\,seeds}}$), defined as the ratio of the number of trigger particles to the sum of near and away-side yields per trigger particle plus one. This ratio increases almost linearly with multiplicity and indicates an onset of a saturation at the highest multiplicities (Fig. 4). In PYTHIA, $N_{\mathrm{uncorrelated\,seeds}}$ is proportional to the number of MPIs and the saturation is related to a steep drop of the probability distribution for the number of MPIs (for example by 4 orders of magnitude between 12 and 24 for PYTHIA6 tune Perugia-0).

Sphericity

Another way to characterise the structure of high-multiplicity pp events is the transverse sphericity. This event-by-event observable can vary between 0 (jet like event) and 1 (particle distribution isotropic in azimuth). In data this observable shows a strong rise as a function of multiplicity until it reaches a plateau value (Fig. 5) [14]. The rise is well reproduced by Monte Carlo event generators. However, at the highest multiplicities they exhibit a turnover to lower sphericity values indicating a stronger (higher p_{T}) jet component as compared to data.

Heavy Flavor yields

An important test of the MPI origin of high multiplicity events is the study of heavy flavour yields as a function of multiplicity. Heavy quarks (c, b) are created in hard processes with a minimum momentum transfer of $Q > 2m_{\mathrm{Q}} \gg \Lambda_{\mathrm{QCD}}$ and they are very rarely created during hadronization of a different parton species. Hence, heavy flavour hadrons are ideal tags for hard processes down to zero p_{T}. Under the assumption that the number of MPIs is proportional to the hard cross section and that the soft particle multiplicity scales with the number of MPIs one expects that the yield from any hard sub-process increases with multiplicity. In ALICE, this behaviour as been verified for D-meson and J/ψ production (see Fig. 6).

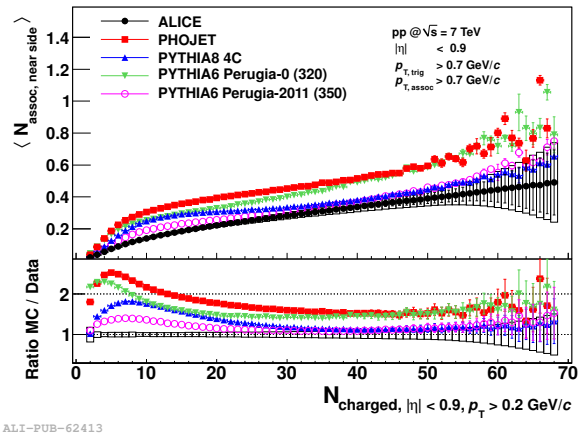

Figure 3. Number of associated particles per trigger particle on the nearside from two-particle azimuthal correlations with $p_{\mathrm{T,trig}}, p_{\mathrm{T,assoc}} > 0.7$ GeV/c in pp collisions at $\sqrt{s} = 7$ TeV [13].

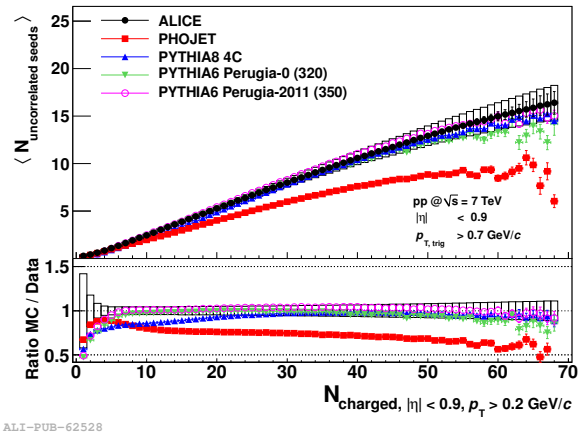

Figure 4. Number of uncorrelated seeds as defined in the text from two-particle azimuthal correlations with $p_{\mathrm{T,trig}}, p_{\mathrm{T,assoc}} > 0.7$ GeV/c in pp collisions at $\sqrt{s} = 7$ TeV [13].

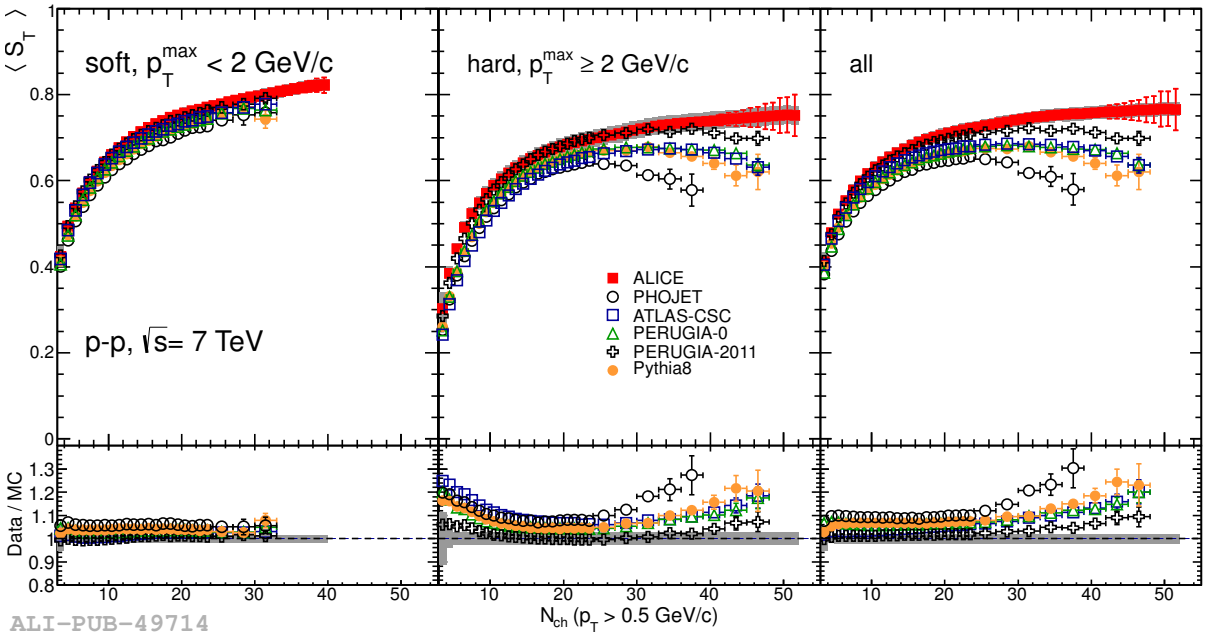

Figure 5. The transverse sphericity as a function of multiplicity in pp collisions at $\sqrt{s} = 7$ TeV for soft events defined as events not containing any particle with $p_{\mathrm{T}} > 2$ GeV/c (left panel), hard events defined as events containing at least one particle with $p_{\mathrm{T}} > 2$ GeV/c (middle panel) and all events (right panel) [14].

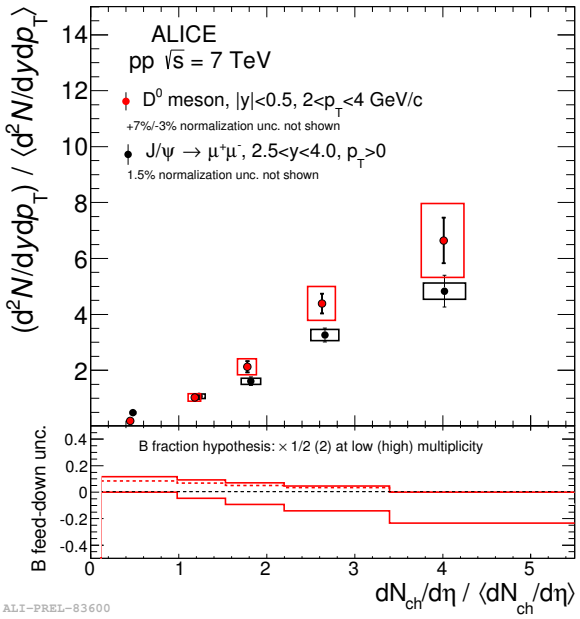
ALICE
pp √s = 7 TeV
D0 meson, |y|<0.5, 2<pT<4 GeV/c
+7%/-3% normalization unc. not shown
J/ψ → μ+μ-, 2.5<y<4.0, pT>0
1.5% normalization unc. not shown
(d2N/dydpT) / ⟨d2N/dydpT⟩
B fraction hypothesis: × 1/2 (2) at low (high) multiplicity
B feed-down unc.
dNch/dη / ⟨dNch/dη⟩
ALI-PREL-83600

Figure 6. D^0-meson self normalised yields vs multiplicity in $2 < p_T < 4$ GeV/c in pp collisions at 7 TeV compared to J/psi $\rightarrow \mu^+\mu^-$. Multiplicity was measured via the number of tracklets (segments formed by two hits in different layers of the pixel detector (SPD) compatible with the reconstructed primary vertex) and is expressed as charged particle density normalised to its mean value.

3. MPIs in p–A

In p–A collisions the number of MPIs is proportional to the number of binary nucleon–nucleon collisions ($N_{\rm coll}$). These MPIs overlap in a transverse collision area similar to the one in pp. However, in comparison to pp, much larger number of MPIs can be reached. It is plausible that effects related to MPIs observed in pp are also relevant in p–A collisions. For example effects due to colour reconnections could be enhanced in p–A due to the larger number of MPIs.

Using the same factorisation approach as in pp and assuming that p–A collisions can be described as an independent superposition of pp collisions one can write for the mean number of MPIs in p–A:

$$\langle n_{\rm hard}\rangle_{\rm pA} = \langle N_{\rm coll}\rangle_{\rm MB}\langle n_{\rm hard}\rangle_{\rm pp} \tag{1}$$

This implies that in general, particle yields from hard processes $Y_{\rm hard}$ normalised by the number of binary collisions scale like

$$\frac{Y_{\rm hard}}{\langle N_{\rm coll}^{\rm cent}\rangle} \propto \frac{\langle n_{\rm hard}\rangle_{\rm pN}}{\langle n_{\rm hard}\rangle_{\rm pp}}. \tag{2}$$

For centrality integrated p–A collisions the ratio $\langle n_{\rm hard}\rangle$(pN)/$\langle n_{\rm hard}\rangle$(pp) is unity. However it is important to note that in this framework it can deviate from unity in centrality event classes. This fact has to be taken into account when studying cold nuclear effects comparing p–A results to the the pp baseline. Two examples, the nuclear modification factor and $\langle p_T\rangle$ as a function of multiplicity are discussed in the following sections.

MPIs and centrality selection in p–A

In general, centrality is defined via estimators that depend monotonically on the number of nucleon-nucleon collisions, e.g. multiplicity and summed energy in a certain pseudo-rapidity range. ALICE employs various sub-detector systems covering disjunct pseudo-rapidity ranges to estimate centrality. $CL1$ is the number of clusters counted in the 2nd layer of the Silicon Pixel Detector covering $|\eta| < 1.4$. $V0A$ and $V0C$ are the summed amplitudes measured by a pair of scintillator arrays covering $2.8 < \eta < 5.1$ and $-3.7 < \eta < -1.7$, respectively. Centrality classes are defined as percentiles of the multiplicity/summed-amplitude distributions.

In order to study the influence of the centrality selection on MPIs in a coherent superposition of p–N collisions we coupled the PYTHIA6 event generator to a p–Pb Glauber MC calculation (G-PYTHIA). For each MC Glauber event PYTHIA is used $N_{\rm coll}$ times to generate $N_{\rm coll}$ independent pp collisions. The resulting charged particle multiplicity distribution in the above mentioned η ranges are used to define centrality classes similar to the ones used in data [15]. Figure 7 shows the average number of hard scatterings ($\langle n_{\rm hard}\rangle$) per binary collision as a function of centrality. In the 20% most central collisions $\langle n_{\rm hard}\rangle$ per $N_{\rm coll}$ is higher than the centrality averaged value and in the most peripheral collisions this ratio is far below this average. As discussed above this bias has consequences for the binary scaling of hard processes. Figure 8 shows the nuclear modification factor $Q_{\rm pPb}^{\rm CL1}$ which is the ratio of the inclusive charged particle spectrum measured in p–Pb to the pp reference scaled by $N_{\rm coll}$. ALICE does not use the conventional notation $R_{\rm pPb}$ to indicate the biased nature of the observable. At high $p_{\rm T}$ (> 6 GeV/c), the centrality dependence of $Q_{\rm pPb}^{\rm CL1}$ reflects the bias on $\langle n_{\rm hard}\rangle$. In addition, in central (peripheral) collisions, $Q_{\rm pPb}^{\rm CL1}$ rises (decreases) with $p_{\rm T}$. This is the consequence of an additional autocorrelation bias. Hard processes contribute themselves to the multiplicity. This contribution increases with the hardness of the scattering. Hence pp events containing a hard scattering are classified more central than an average collision. At high $p_{\rm T}$ the G-PYTHIA model of independent collisions describes the data well. Global particle production scales with the number of participants and as we will see later in the low- and intermediate $p_{\rm T}$ region effects reminiscent of collective behaviour in A–A are observed. Hence, as expected our simple model does not describe the low- and intermediate $p_{\rm T}$ region. One important observation in this region that will be discussed in the next section is the increase of the average transverse momentum $\langle p_{\rm T}\rangle$ with multiplicity.

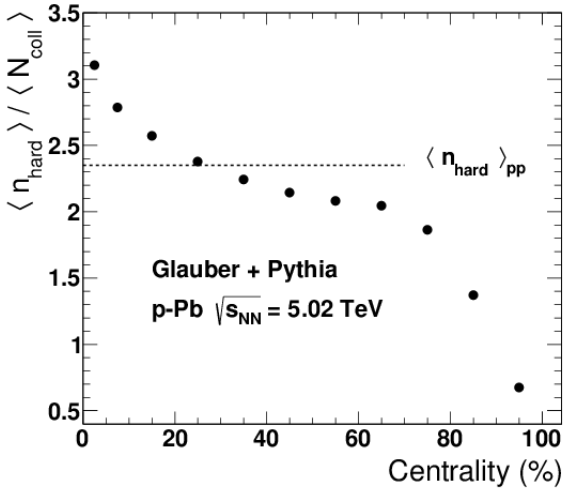

Figure 7. Average number of hard collisions per binary p–nucleon collision as a function of centrality from the G-PYTHIA calculation described in the text.

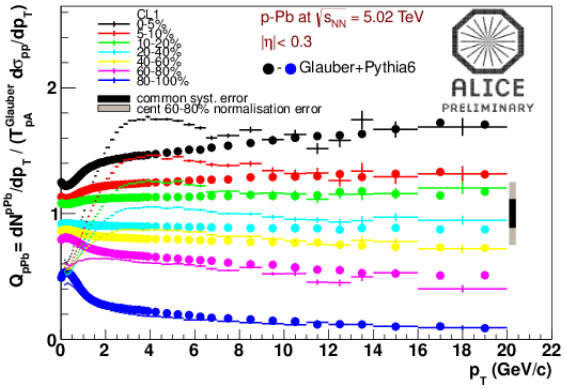

Figure 8. $Q_{\rm pPb}$ for the CL1 centrality estimator compared to the G-PYTHIA calculation as described in the text for p–Pb collisions at $\sqrt{s_{\rm NN}} = 5.02$ TeV .

Multiplicity dependent measurements in p–Pb

Figure 2 shows the average transverse momentum as a function of multiplicity for pp collisions at $\sqrt{s} = 7$ TeV, p–Pb at $\sqrt{s_{\rm NN}} = 5.02$ TeV and Pb–Pb at $\sqrt{s_{\rm NN}} = 2.76$ TeV [11]. From measurements of, $\langle p_{\rm T}\rangle(N_{\rm ch})$ in pp at several energies we expect that the $\sqrt{s}$-dependence of this

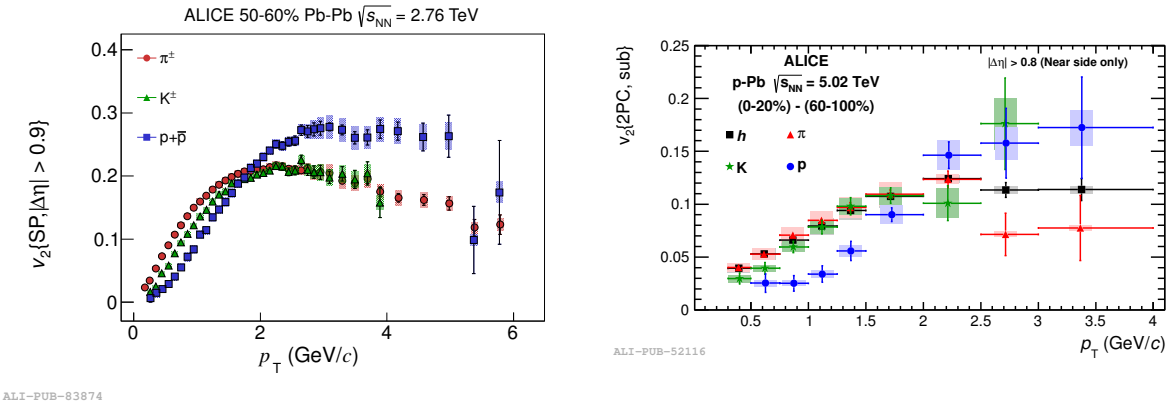

Figure 9. For hadrons, pions, kaons and protons: (left panel) $v_2(p_{\mathrm{T}})$ for mid-central Pb–Pb collisions [24] and (right panel) $v_2\{2\mathrm{PC}, \mathrm{sub}\}(p_{\mathrm{T}})$ from 2-particle correlations in the 0–20% multiplicity class after subtraction of the correlation from the 60–100% multiplicity class [26].

observable is weak and, hence, we assume the results for the three collision systems can be directly compared. With respect to Pb–Pb, in p–Pb, $\langle p_{\mathrm{T}} \rangle$ shows a much stronger increase with multiplicity following the pp data up to $N_{\mathrm{ch}} = 14$. Note that multiplicities around 14 correspond to typical p–Pb collision, whereas pp collisions at this multiplicity are already strongly biased ($N_{\mathrm{ch}} > 14$ corresponds to 50% (10%) of the p–Pb (pp) cross-section). As discussed in the introduction, in pp this rise cannot be explained by an independent superposition of multiple parton scatterings and can be attributed to the effect of colour re-connections between strings. Similar to the model described above one can try to describe the rise of $\langle p_{\mathrm{T}} \rangle$ in p–Pb collisions by a superposition of parton scatterings from an incoherent superposition of p–nucleon collisions [16, 11] (see Fig. 2 middle panel, solid line). The observed rise of $\langle p_{\mathrm{T}} \rangle$ is significantly stronger than expected suggesting that also in this case effects from interactions between MPIs like colour re-connections are at work. The EPOS generator which includes hydrodynamic collective flow can reproduce the p–Pb data, however, it fails to describe peripheral Pb–Pb collisions. ALICE has also measured the multiplicity dependence of $\langle p_{\mathrm{T}} \rangle$ for identified particles (π, K, p, Λ). Here, a clear mass ordering $\langle p_{\mathrm{T}} \rangle_{\Lambda} > \langle p_{\mathrm{T}} \rangle_{\mathrm{p}} > \langle p_{\mathrm{T}} \rangle_{\mathrm{K}} > \langle p_{\mathrm{T}} \rangle_{\pi}$ is observed [18], which is an indication for collective expansion with a common velocity field. The same kind of mass ordering is also qualitatively expected from colour re-connections [17].

In heavy-ion collisions, the increase of $\langle p_{\mathrm{T}} \rangle$ and its mass ordering find their natural explanation in the collective radial expansion of the system [19]. This scenario can be corroborated in the blast-wave framework with a simultaneous fit to all particles for each multiplicity bin [20]. From the fit one obtains the mean radial velocity $\langle \beta \rangle$ and kinetic freeze-out temperature T_{kin}. It is found that the trend of T_{kin}-$\langle \beta \rangle$ as a function of multiplicity is very similar in p–Pb and Pb–Pb collisions [18]. The same trend, albeit at a 30% smaller T_{kin}, can be also reproduced with pp collisions simulated by PYTHIA8 when colour reconnections are included.

Two-particle angular correlations in p–Pb

The strongest evidence for collective effects in p–Pb results from the study of triggered 2-particle angular correlations in the azimuthal ($\Delta\varphi$) and pseudo-rapidity ($\Delta\eta$) differences. These correlations show symmetric ridge like-structures elongated in $\Delta\eta$ at the near-side ($\Delta\varphi = 0$) and away-side ($\Delta\varphi = \pi$) of the trigger particle [21, 22, 23]. They are very similar to the momentum anisotropy observed in Pb–Pb [24], where the effect is attributed to collectivity (flow) (Fig. 9) [26]. Whereas these correlations can be explained by hydrodynamic flow or models based on the

Color Glass Condensate [25], the above mentioned MPI Monte Carlo models based on colour re-connections are not yet able to describe this observation.

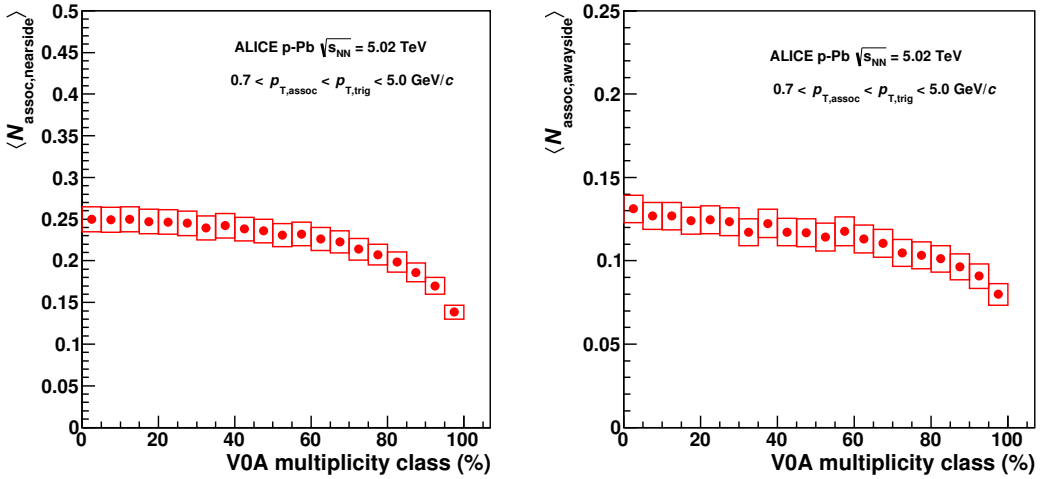
ALICE p-Pb $\sqrt{s_{NN}}$ = 5.02 TeV
0.7 < $p_{T,assoc}$ < $p_{T,trig}$ < 5.0 GeV/c
$\langle N_{assoc,nearside} \rangle$
V0A multiplicity class (%)
ALICE p-Pb $\sqrt{s_{NN}}$ = 5.02 TeV
0.7 < $p_{T,assoc}$ < $p_{T,trig}$ < 5.0 GeV/c
$\langle N_{assoc,awayside} \rangle$
V0A multiplicity class (%)

Figure 10. Near-side (left) and away-side (right) per-trigger yield as a function of V0A multiplicity class in p–Pb collisions at $\sqrt{s_{\rm NN}} = 5.02$ TeV with $0.7 < p_{\rm T,assoc} < p_{\rm T,trig} < 5.0$ GeV/c [27].

Whereas $\langle p_{\rm T} \rangle$ and long-range correlations are sensitive to collective effects, possible local changes to parton fragmentation can be studied by jet-like short range correlations in $\Delta\eta - \Delta\varphi$. Figure 10 shows the near-side and away-side per trigger yields as a function of the V0A multiplicity class in p–Pb collisions at $\sqrt{s_{\rm NN}} = 5.02$ TeV [27]. Contrary to the strong event activity dependence observed for $\langle p_{\rm T} \rangle$ and for the long-range correlations, the yields measured in jet-like correlations stay unmodified over a wide range of V0A multiplicity percentile. Only for the lowest multiplicities ($> 70\%$) a significant decrease of the yields is observed. It can be expected that this observation puts new constraints on models implementing coherence effects between MPI or collective hadronization.

3.1. Summary

ALICE has explored the rich phenomenology of MPI in pp collisions. In particular, the study of the multiplicity dependence of jet-like azimuthal two-particle correlations shows in a quite direct way that, in agreement with Monte Carlo simulations, high multiplicity pp events can be understood as a superposition of semi-hard scatterings.

Studies of observables as a functions of multiplicity have been extended to p–Pb. Phenomena which are in nucleus–nucleus well established as the consequence of collective hydrodynamic flow are observed. The observed increase of $\langle p_{\rm T} \rangle$ and its mass ordering has been also observed in pp where it can be attributed to colour re-connections between strings formed by multiple parton-parton interactions. It can be speculated that this effect plays also an important role in p–Pb where the MPIs overlap in a transverse region similar to pp. The EPOS Monte Carlo generator which includes collective fragmentation effects via hydrodynamic flow for small collision systems is in agreement with the pp and p–Pb data. Hydrodynamic flow is also a natural explanation for the symmetric double-ridge structure observed in p–Pb. With the aim to get more insight into the possible influence of these effects on parton fragmentation, ALICE has studied jet-like angular correlations at low $p_{\rm T}$ as a function of multiplicity in p–Pb. Surprisingly the fragmentation properties expressed as the yield associated to a trigger particles stays constant

over a wide range of multiplicities. Future model comparisons will show whether these findings can be used to further constrain coherent fragmentation effects.

References

[1] Sjöstrand T and van Zijl M 1987 *Phys. Rev.* D **36** 2019
[2] Sjostrand T and Skands P Z 2004 *JHEP* **0403** 053
[3] Sjostrand T and Skands P Z 2005 *Eur. Phys. J.* C **39** 129
[4] Bahr M, Butterworth J M and Seymour M H 2009 *JHEP* **0901** 065
[5] Sjostrand T, Mrenna S and Skands P Z 2006 JHEP **0605** 026
[6] Sjostrand T, Mrenna S and Skands P Z 2008 *Comput. Phys. Commun.* **178** 852
[7] Sjostrand T and van Zijl M 1987 *Phys. Lett.* B **188** 149
[8] Abelev B B *et al.* (ALICE Collaboration) 2012 *JHEP* **1207** 116
[9] Skands P Z and Wicke D 2007 *Eur. Phys. J.* C **52** 133
[10] Gieseke S, Rohr C and Siodmok A, 2012 *Eur. Phys. J.* C **72** 2225
[11] Abelev B B *et al* (ALICE collaboration) 2013 *Phys. Lett.* B **727** 371-380
[12] Pierog T *et al.* arXiv:1306.0121 [hep-ph].
[13] Abelev B B *et al.* (ALICE Collaboration) 2013 *JHEP* **1309** 049
[14] Abelev B B *et al.* (ALICE Collaboration) 2012 *Eur. Phys. J.* C **72** 2124
[15] Morsch A (ALICE Collaboration) 2014 *J. Phys. Conf. Ser.* **509** 012021
[16] Bzdak A and Skokov V *Phys. Lett.* B **726** (2013) 408
[17] A. Ortiz Velasquez *et al. Phys. Rev. Lett.* **111** (2013) 4, 042001
[18] Abelev B B *et al* (ALICE Collaboration) 2014 *Phys. Lett.* B **728** 25-38
[19] Heinz U W 2004 Concepts of heavy ion physics, CERN-2004-001-D
[20] Schnedermann E, Sollfrank J and Heinz U W 1993 *Phys. Rev.* C **48** 2462
[21] Chatrchyan S (CMS Collaboration) *et al* 2013 *Phys. Lett.* B **718** 795
[22] Abelev B B *et al* (ALICE Collaboration) 2013 *Phys. Lett.* B **719** 29-41
[23] Aad G *et al* (ATLAS Collaboration) 2013 *Phys. Rev. Lett.* **110** 182302
[24] Abelev B B *et al.* (ALICE Collaboration) 2014 arXiv:1405.4632 [nucl-ex]
[25] Dusling K and Venugopalan R 2013 *Phys. Rev.* D **87** 5 054014
[26] Abelev B B *et al.* (ALICE Collaboration) 2013 *Phys. Lett.* B **726** 164-177
[27] Abelev B B *et al.* (ALICE Collaboration) 2014 arXiv:1406.5463 [nucl-ex].